

Full Research Paper

Assessing Steady-state Fluorescence and PRI from Hyperspectral Proximal Sensing as Early Indicators of Plant Stress: The Case of Ozone Exposure

Michele Meroni¹, Micol Rossini^{1,*}, Valentina Picchi^{2,3}, Cinzia Panigada¹, Sergio Cogliati¹, Cristina Nali³ and Roberto Colombo¹

¹ Remote Sensing of Environmental Dynamics Lab., DISAT, University of Milan-Bicocca, piazza della Scienza 1, 20126 Milano, Italy. E-mails: michele.meroni@unimib.it; cinzia.panigada@unimib.it; s.cogliati3@campus.unimib.it; roberto.colombo@unimib.it

² CNR, Plant Virology Institute, Milan Unit, Italy. E-mail: valentina.picchi@unimi.it

³ Department of Tree Science, Entomology and Plant Pathology “G. Scaramuzzi”, University of Pisa, Italy. E-mail: cnali@agr.unipi.it

* Author to whom correspondence should be addressed. E-mail: micol.rossini@unimib.it

Received: 31 January 2008 / Accepted: 11 March 2008 / Published: 13 March 2008

Abstract: High spectral resolution spectrometers were used to detect optical signals of ongoing plant stress in potted white clover canopies subjected to ozone fumigation. The case of ozone stress is used in this manuscript as a paradigm of oxidative stress. Steady-state fluorescence (Fs) and the Photochemical Reflectance Index (PRI) were investigated as advanced hyperspectral remote sensing techniques able to sense variations in the excess energy dissipation pathways occurring when photosynthesis declines in plants exposed to a stress agent. Fs and PRI were monitored in control and ozone fumigated canopies during a 21-day experiment together with the traditional Normalized Difference Vegetation Index (NDVI) and physiological measurements commonly employed by physiologists to describe stress development (i.e. net CO₂ assimilation, active fluorimetry, chlorophyll concentration and visible injuries). It is shown that remote detection of an ongoing stress through Fs and PRI can be achieved in an early phase, characterized by the decline of photosynthesis. On the contrary, NDVI was able to detect the stress only when damage occurred. These results open up new possibilities for assessment of plant stress by means of hyperspectral remote sensing.

Keywords: Vegetation stress; hyperspectral remote sensing; PRI; passive fluorescence.

1. Introduction

Environmental stresses come from a variety of factors which, besides very specific effects, often limit the potential growth of vegetation. Plants respond to the onset of the stress condition with a variety of coping mechanisms [1] aimed at compensating the adverse effects of the stress. Afterwards, if the stressor is not removed, the overload of these mechanisms may lead to a progressive loss of plant vitality causing severe reductions of plant productivity.

The detection of an ongoing stress in its early phase is critical information required for taking action for its mitigation. For example, the early detection of drought or nutrient deficiency in crops would allow farmers to manage water or fertilization supplies in order to avoid a production loss.

Remote sensing (RS) offers a unique opportunity for mapping vegetation stress and monitoring its time course. From a RS point of view, the state of stress has been expressed by changes of optical signals (e.g. Normalized Difference Vegetation Index, NDVI) related to some canopy variables (e.g. leaf area index, LAI, and chlorophyll concentration) [2-6]. However, when canopy chlorophyll concentration or total leaf area are affected by the stress, damage to the plant has already occurred, and plant status is compromised.

In an earlier stage of the stress and before damage has occurred, photosynthesis declines. In such conditions, the absorbed light exceeds the photosynthetic demand. This light surplus is dissipated by plants to avoid light-induced oxidative damage. Two dissipation processes compete for this energy surplus: chlorophyll fluorescence and non-photochemical quenching, NPQ [7]. Fluorescence is the process by which the light energy absorbed by chlorophyll pigments at one wavelength is re-emitted at a different wavelength [8]. NPQ involves acidification of the thylakoid lumen, the operation of the xanthophyll cycle and specific components of the antenna [8] for the thermal dissipation of excess energy.

As a result, when a stress factor depresses the rate of photosynthesis, the excess energy is mostly diverted from chlorophyll to xanthophyll cycle pigments as part of NPQ with a related reduction in fluorescence. Hyperspectral sensors (i.e. high number of narrow bands) nowadays allow the remote detection of the variation of these energy dissipation processes by sun-induced steady-state fluorescence (Fs) and the Photochemical Reflectance Index (PRI). The Fs signal emitted by plants can be detected passively by examination of the faint radiance in very narrow dark lines of the solar incident irradiance (Fraunhofer lines), caused by atmospheric absorptions. Fs detection requires a spectroradiometer with a subnanometer spectral resolution since the exploitable Fraunhofer lines are typically 0.5 to 2 nm wide, while PRI can be investigated by traditional portable high spectral resolution sensors (2 to 5 nm).

Background information on hyperspectral techniques used in this work to retrieve these variables is given in Section 2.

The objective of this research was to investigate the feasibility of detecting stress in its early phase using Fs and PRI at the canopy level by means of hyperspectral sensors. A case study of ozone (O₃) stress development on potted white clover canopies is presented. Ozone toxicity is due to the induced imbalance between the production and the scavenging of reactive oxygen species (ROS) in plant cells. This imbalance, referred to as oxidative stress, is caused by a variety of adverse abiotic (i.e. high light, drought, low temperature, high temperature, mechanical stress) or biotic (i.e. pathogen attack) stress

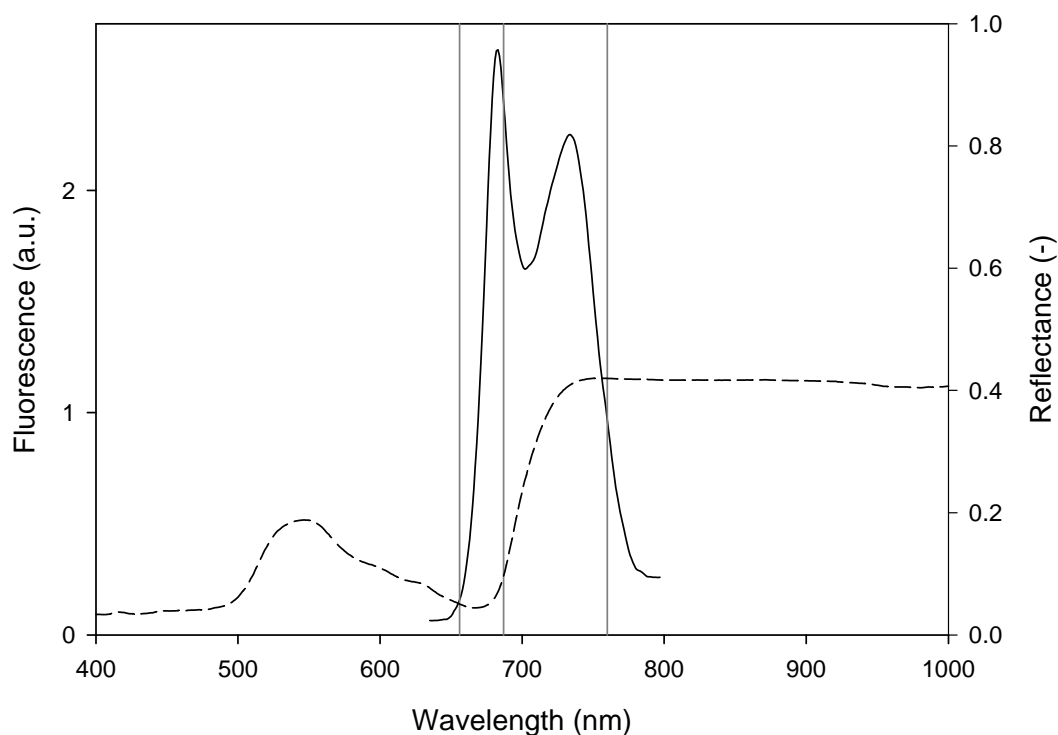
conditions [9, 10]. Therefore, the case of O₃ exposure is used in this work as a paradigm of stress development.

2. RS of energy dissipation pathways

2.1 Steady-state fluorescence

Under natural solar light, plants fluoresce continuously adding a weak emitted signal (about 1% of the absorbed light in the visible part of the spectrum), the so-called sun-induced steady-state fluorescence (Fs), to reflected solar radiation. Fs can be quantified passively (i.e. without artificial excitation sources) in the Fraunhofer lines in which solar incident irradiance is strongly attenuated. In the visible and near-infrared, the solar irradiance spectrum at ground level exhibits three main bands which have been exploited for this purpose [e.g. 11, 12]: the solar atmosphere hydrogen absorption band, H α (656.3 nm) and the terrestrial atmosphere oxygen absorption bands B (687 nm) and A (760 nm). The oxygen absorption bands have been used more extensively than the H α because they are spectrally closer to the peaks of chlorophyll fluorescence emission spectra positioned at about 690 and 740 nm as shown in Figure 1, where the reflectance and the chlorophyll fluorescence spectra of a green leaf are depicted.

Figure 1. Fluorescence emission spectrum of a white clover leaf excited with a tungsten halogen light source filtered with a short-pass filter blocking the light in the emission region 650-800 nm (continuous curve). Reflectance spectrum of the same leaf (dashed curve). Position of the hydrogen absorption H α (656 nm) and oxygen absorption A (760 nm) and B (687 nm) bands (grey vertical lines).



The oxygen A band was exploited in this work because it is larger (in terms of bandwidth) and deeper (in terms of attenuation with respect to *continuum*) than the B band [e.g. 13].

Details of the internal structure and frequency features of the A band can be observed in the incident solar radiance spectrum (L^i , continuous black curve in Figure 2) collected with a very high spectral resolution spectrometer.

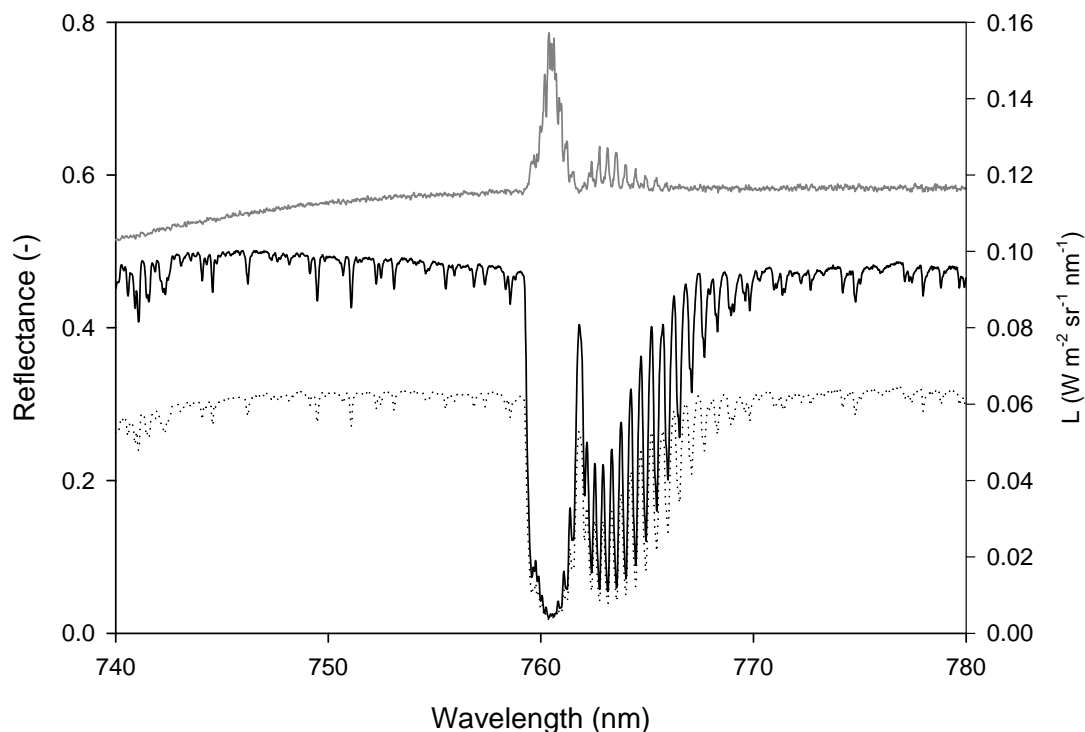
The radiance upwelling from the vegetated target (L^s , dashed curve in Figure 2) at a given wavelength can be expressed as the sum of a reflected and an emitted flux (i.e. fluorescence):

$$L^s(\lambda) = \rho(\lambda) L^i(\lambda) + F_s(\lambda) \quad (1)$$

where ρ is the actual reflectance (free of the emission component).

Figure 2 also demonstrates that the reflectance, computed as the ratio of the radiance upwelling from the target and the radiance incident on it (i.e. L^s/L^i), is indeed an apparent reflectance because it is affected by fluorescence as is clearly shown by the in-filling of the A band which causes the peak at 760.62 nm.

Figure 2. Incident solar radiance (L^i , black continuous curve) and radiance upwelling from a vegetated target (L^s , black dashed curve) around the A band. The grey curve is the resulting apparent reflectance. Measurements were collected over a white clover canopy with a HR4000 (OceanOptics, USA) characterized by a full width at half maximum (FWHM) of 0.13 nm.



In the A band (up to more than 90% of attenuation), fluorescence can be detected by measuring to what extent the “well” shown in Figure 2 is filled by fluorescence relative to the *continuum* [14]. This technique forms the basis of the Fraunhofer Line-Depth (FLD) method for the estimation of fluorescence [11]. The method requires the measurement of L^i and L^s in two narrow spectral bands (at

the border and at the bottom of the well). Fluorescence is then computed by the determined linear system formed with equation (1) evaluated at these two wavelengths, on the assumption that the fluorescence flux and the reflection coefficient are constant [e.g. 11, 12, 15].

However, considering the shape of fluorescence and reflectance curves in the A band region (Figures 1 and 2) it appears that the approximation of constant F_s and ρ is not appropriate. A modelling approach overcoming this limitation was proposed by Meroni and Colombo [13]. This approach requires a large number of spectral channels within a single Fraunhofer line (as shown in Figure 2) and assumes linearity for ρ and F_s in the A band region. The upwelling radiance is therefore expressed as follows:

$$L^s(\lambda_0 + \Delta\lambda) = \left[\rho(\lambda_0) + \frac{d\rho}{d\lambda} \Delta\lambda \right] L^i + F_s(\lambda_0) + \frac{dF_s}{d\lambda} \Delta\lambda \quad (2)$$

where λ_0 is the lower wavelength limit of the spectral range considered and $d/d\lambda$ is the derivative with respect to wavelength. With the large number of spectral observations provided by very high spectral resolution spectrometers, an overdetermined bilinear system can be formed with equation (2). The four unknowns (i.e. gain and offset of the linear $\rho(\lambda)$ and $F_s(\lambda)$ functions) are estimated solving the system with the Ordinary Least Square (OLS) for bilinear equations.

2.2 Photochemical Reflectance Index (PRI)

Non-photochemical quenching is a process that thermally dissipates the absorbed light energy in photosystem II (PSII) that exceeds the photosynthetic demand, thus minimizing light-induced oxidative damage. Although the exact mechanisms of NPQ are not completely understood, recent experimental works support the hypothesis that zeaxanthin formation, via the xanthophyll cycle pigments, is responsible for the majority of dissipation of the excess excitation energy [16-19]. Under excess light, violaxanthin is converted rapidly via the intermediate antheraxanthin to zeaxanthin (i.e. de-epoxidation), and this reaction is reversed under low light levels (i.e. epoxidation) [20].

The interconversion of the xanthophyll cycle pigments can be detected in leaves through a change in the absorbance at 505-515 nm [21] or in the reflectance at 531 nm [22].

The Photochemical Reflectance Index (PRI) was proposed by Gamon *et al.* [23] using two wavelengths: 531 nm, which is affected by xanthophyll de-epoxidation, and 570 nm which is the reference waveband. The PRI is formulated as follows:

$$PRI = (R_{531} - R_{570}) / (R_{531} + R_{570}) \quad (3)$$

where R refers to the narrow-band reflectance centered on the stated wavelength. PRI values decrease as the xanthophyll de-epoxidation state increases.

3. Materials and methods

3.1 Plant material and ozone exposure

White clover plants (*Trifolium repens* L. cv. Regal) were grown from cuttings originally supplied by the Coordination Centre of the ICP Vegetation at the Centre for Ecology and Hydrology (Bangor, UK). One cutting per pot (1 dm³) was firstly placed in a controlled environment facility at a temperature of 20±1°C, a relative humidity (RH) of 85±5% and a photosynthetic photon flux density (PPFD) at plant height of 500 µmol photons m⁻² s⁻¹ provided by incandescent lamps, during a 14 h photoperiod. The substrate was a mix of mature manure, organic soil and peat, all added with a slow-release N–P–K (8:10:45) fertiliser. After three weeks, nine plants were then transplanted in 15 litre volume pots with a surface diameter of 35 cm to create a vegetation canopy. The plants were then maintained under the same conditions in the growth chamber above described for one month. Experiment started on the 19th of September 2006 when potted plants showed a dense and full canopy.

Treated plants were exposed to chronic O₃ fumigation (100 ppb O₃, 5 h d⁻¹) for three weeks in a controlled environment fumigation facility described in Nali *et al.* [24]. Control plants were maintained under the same experimental conditions and exposed to charcoal-filtered air.

Ozone exposure was expressed in terms of AOT40 (Accumulated exposure Over a Threshold of 40 ppb) which is defined as the sum of the differences between the hourly mean O₃ concentration (in ppb) and 40 ppb for each hour when the concentration exceeds 40 ppb, accumulated during daylight hours [25].

3.2 Data collection

Meteorological, physiological and spectral measurements were collected outdoors under natural solar illumination at 10:30 a.m. (solar time), as suggested by Amoros-Lopez *et al.* [26], during six field campaigns conducted from day 0 (before the beginning of fumigation) to day 21 of the fumigation treatment. The onset of stress was monitored daily from day 0 to 4. The last field campaign was conducted after 21 days of fumigation in order to investigate the damage phase of stress.

Spectral measurements were acquired in clear sky conditions over three areas of the canopy. Subsequently, six fully expanded leaves from separate plants in the upper portion of the canopy were used for physiological measurements. Leaf dry matter content and LAI were destructively measured at the end of the experiment.

3.2.1 Spectral measurements

Two HR4000 holographic grating spectrometers (OceanOptics, USA) characterised by different spectral resolutions were used in the experiment. Both sensors employ a 3648-element linear CCD array (Toshiba TCD1304AP, Japan). Spectrometer 1 was used to estimate Fs at the oxygen A band. Spectrometer 2 was used for the computation of PRI and NDVI. Sensor characteristics are reported in Table 1.

Spectrometers were calibrated before the field campaign with known standards (wavelength and radiance calibration sources). Measurements were acquired using bare fiber optics with an angular

field of view of 25° to measure from nadir a circular area of the canopy of 10 cm in diameter. The fibers were mounted on a rotating arm in order to observe three areas per each canopy.

A calibrated white reference panel (50x50 cm 90% reflectance, Optopolymer GmbH, Germany) was employed to estimate incident irradiance. The field spectroscopy technique referred to as ‘single beam’ [27] was employed: target measurements are ‘sandwiched’ between two reflectance standard panel measurements made a few seconds apart. The radiance of the reference panel at the time of the target measurement is estimated by linear interpolation. This technique is based on the assumption that incident irradiance varies linearly between the two reference panel measurements.

Table 1. Spectrometer technical information.

	FWHM (nm)	Sampling interval (nm)	Spectral range (nm)
Spectrometer 1	0.13	0.02	707-805
Spectrometer 2	2.8	0.24	350-1050

For every spectral acquisition, 4 and 15 scans (spectrometers 1 and 2, respectively) were averaged and stored as a single file. Additionally, a dark current measurement was collected for every subset of three acquisitions. Spectrometers were housed in a Peltier thermally insulated box (model NT-16, Magapor, Zaragoza, Spain) keeping the internal temperature at 25°C in order to reduce dark current drift. Spectral data were acquired and processed with dedicated software [28]. Processing of raw data included: correction for CCD detector nonlinearity, correction for dark current and dark current drift using optically black pixels, wavelength calibration and linear resampling, radiance calibration, incident irradiance computation by linear interpolation of two white reference measurements.

The spectral interval used for fluorescence estimation in the A band (F_{S760}) according to equation (2) was set to 759.00 - 767.76 nm for a total of 439 channels used.

An index of fluorescence efficiency at 760 nm, normalized fluorescence (NF_{S760}), was calculated as the ratio between F_{S760} and the radiation incident in a nearby 15 nm region of the *continuum* [29].

In order to estimate xanthophyll-related NPQ, the PRI was computed according to equation (3).

Furthermore, the traditional optical vegetation index NDVI, potentially capable of detecting the damage phase, was calculated as follows:

$$NDVI = (R_{800} - R_{680}) / (R_{800} + R_{680}) \quad (4)$$

3.2.2 Physiological measurements and meteorological dataset

The leaf net CO₂ assimilation rate was measured with a portable infrared gas analyzer (CIRAS-1, PP-Systems, Stotfold, UK) equipped with a Parkinson leaf chamber (details are reported in [24]).

Measurements were performed at ambient CO₂ concentrations and illumination. Active fluorimetry measurements were acquired with a portable fluorimeter (PAM-2000, Walz, Effeltrich, Germany) under natural illumination. The quantum yield of electron transport through PSII ($\Delta F/F_m'$) was determined as $(F_m' - F_t)/F_m'$ [30], where F_m' is the maximum fluorescence of the light-adapted sample and F_t is the chlorophyll fluorescence yield under natural illumination. The maximum photochemical efficiency of dark-adapted samples (F_v/F_m , where F_m is the maximum fluorescence and F_v is the difference between the maximum and the baseline fluorescence) was measured before dawn.

Relative chlorophyll concentration was estimated by a SPAD 502 (Minolta, Tokyo - Japan) leaf chlorophyll meter (three readings per leaf).

In addition, destructive measurements of LAI were performed at the end of the experiment with a portable area meter (Model LI-3000, Li-Cor). Leaf dry matter content was calculated by drying the leaves at 80°C in an oven until constant weight (dry weight) was reached.

Assessment of visible O₃ injury was carried out in terms of percentage of injured leaves, according to the ICP (International Cooperative Programme) Vegetation Experimental Protocol [31].

During measurements, air temperature and RH (Rotronic, Germany), total and diffuse incident PPFD (BF3, Delta-T, UK), were continuously logged (DL2, Delta-T, UK). Ambient temperature ranged from 18 to 27°C, RH from 62 to 81% and incoming PPFD from 900 to 1400 $\mu\text{mol m}^{-2} \text{s}^{-1}$.

3.3 Statistical analysis

Comparisons between control and treated plant variables were performed according to Student's *t*-test. The level of statistical significance was set at $P = 0.05$ (ns : $P > 0.05$; * : $P \leq 0.05$; ** : $P \leq 0.01$; *** : $P \leq 0.001$). Physiological measurements are expressed as the mean of measurements collected on single leaves (six leaves per thesis) while spectral measurements are expressed as the mean of measurements acquired on three areas of the canopy.

4. Results and Discussion

Time series of the investigated variables measured at 10:30 a.m. (solar time) were generated in order to analyze differences between control and treated plants as the stress developed. Physiological and spectral variables monitored over the 21 days experiment are shown in Figures 3 and 4, respectively.

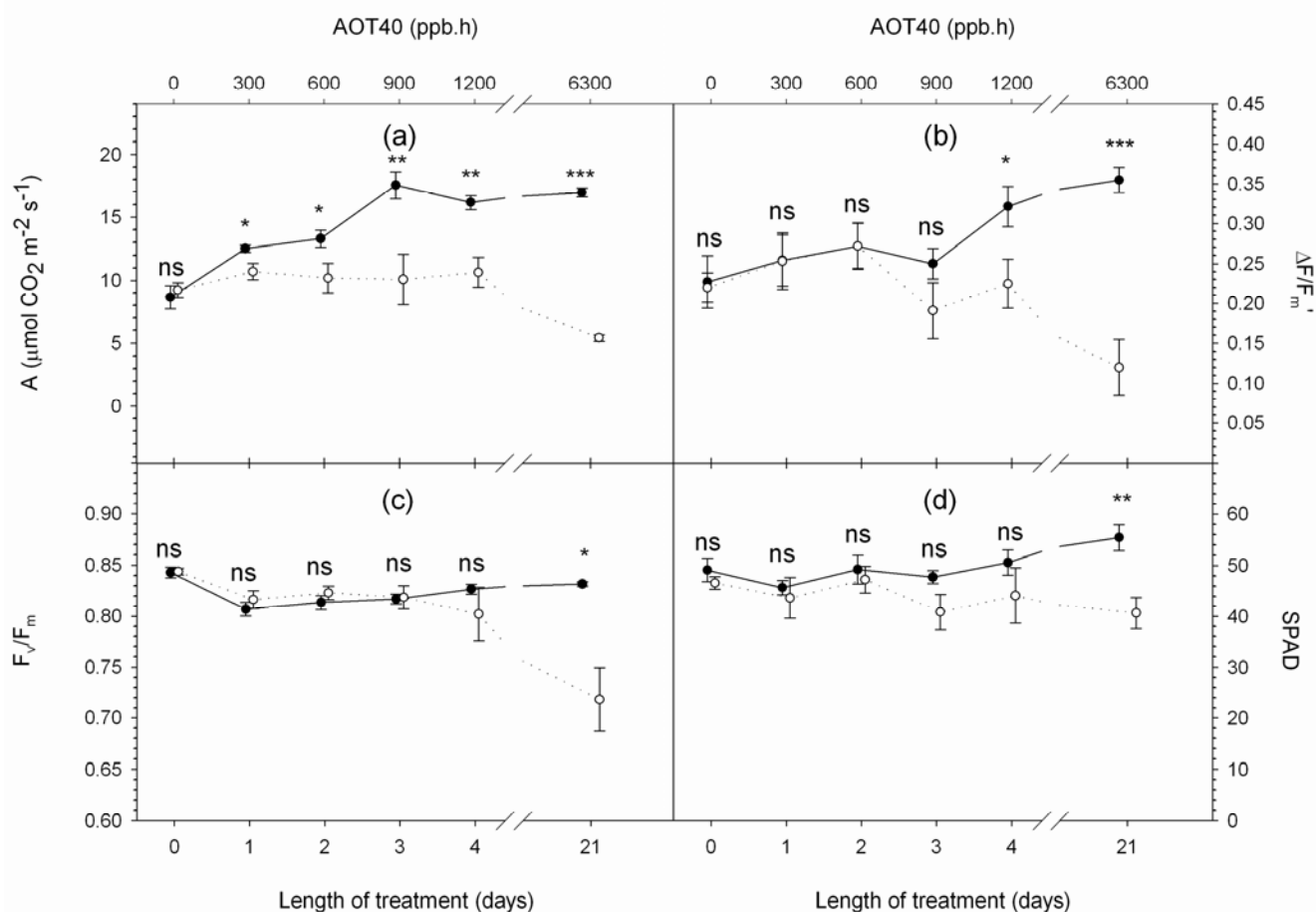
On day 0, both physiological and spectral measurements indicated that control and treated plants were in similar vigour before fumigation (i.e. no significant difference observed in any variable).

Afterwards, physiological measurements suggested that treated plants experienced increasing stress due to chronic O₃ fumigation. Upon exposure to O₃, plants showed lower photosynthetic rates with respect to controls (Figure 3a), evidenced by a significant decrease in the net CO₂ assimilation rate from day 1 and active fluorescence quantum yield ($\Delta F/F_m'$) from day 4 (Figure 3b). These observations are in agreement with other studies and show that O₃ is able to impair photosynthetic activity, reducing carboxylation efficiency and altering the light reactions of photosynthesis, decreasing the electron transport rate between the two photosystems [32-37].

A significant decrease in maximum photochemical efficiency of dark-adapted samples (F_v/F_m), which is commonly considered a sign of photoinhibition [38] and has frequently been observed in

plants subjected to chronic O₃ fumigation [39-41], was experienced by treated plants after 21 days of fumigation (Figure 3c), when visible injury appeared as sparse dark stipples on 10% of treated leaves and the relative chlorophyll concentration was significantly reduced (Figure 3d). Observations of chlorophyll degradation connected to senescence-like mechanisms have been reported as a common effect of O₃ exposure. According to Castagna *et al.* [42], this degradation may be due to damage (chlorophyll breakdown caused by O₃-derived ROS) or acclimatization (chlorophyll breakdown as plant strategy to avoid excessive light interception in the antennae).

Figure 3. Time series of physiological variables measured at 10:30 a.m. (solar time): (a) A, net CO₂ assimilation rate ($\mu\text{mol CO}_2 \text{ m}^{-2} \text{ s}^{-1}$); (b) $\Delta F/F_m'$, fluorescence quantum yield; (c) F_v/F_m , maximum photochemical efficiency of dark-adapted samples; (d) SPAD, relative leaf chlorophyll concentration. Full and empty dots refer to control and treatment samples respectively. Values represent means \pm SE (n = 6). Comparison between means was performed according to Student's t-test (ns : P > 0.05; * : P \leq 0.05; ** : P \leq 0.01; *** : P \leq 0.001).



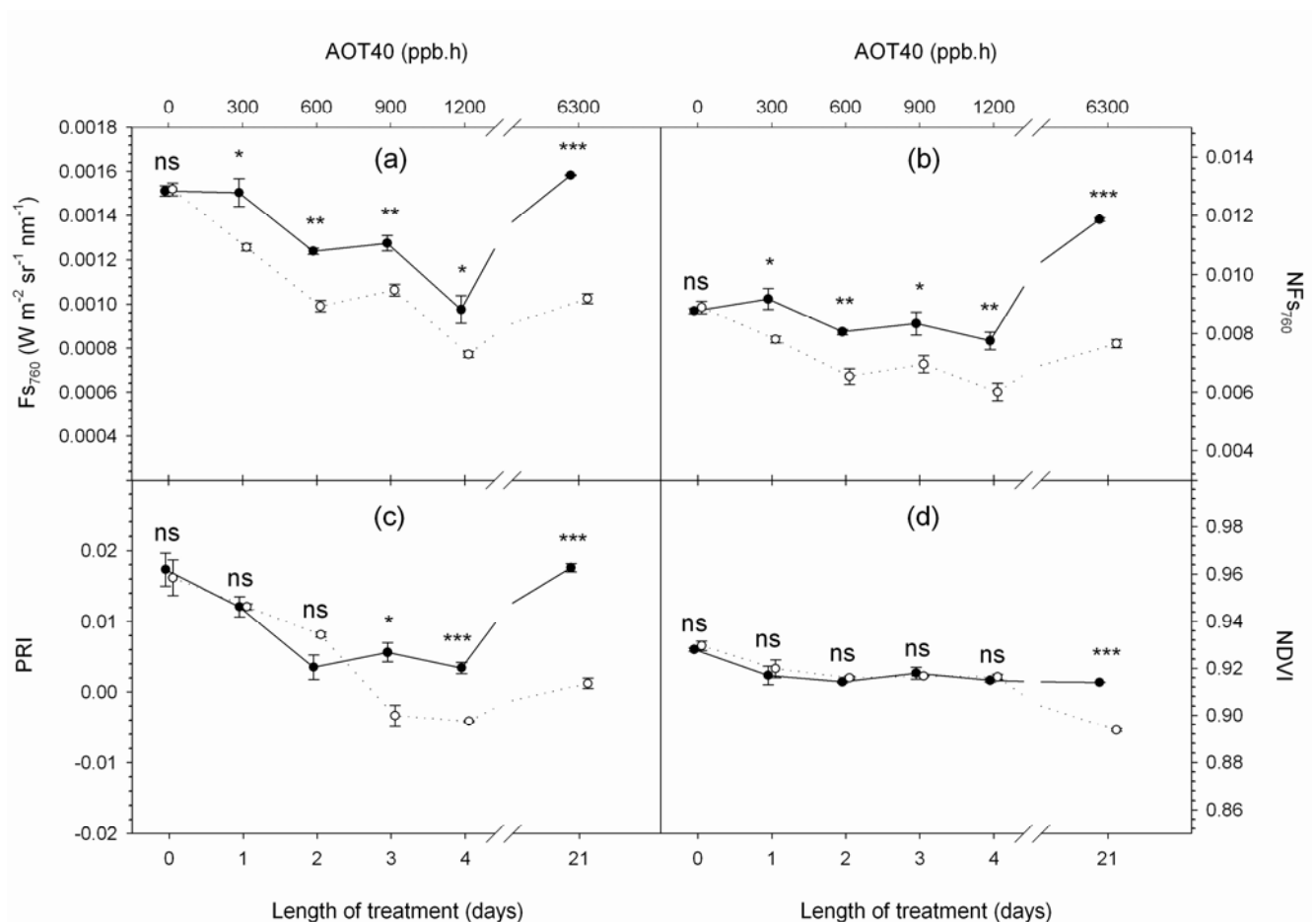
Physiological measurements illustrated the evolution of vegetation response to a stress agent: the early phase of stress (i.e. photosynthesis decline) is followed by the damage phase characterized by senescence-like mechanisms manifested as chlorophyll degradation. This stress gradient allowed us to investigate the capability of remotely sensed Fs and PRI to monitor stress development.

Fs variables derived from very high resolution data, FS_{760} and NFS_{760} , responded immediately to O₃ exposure (Figures 4a and b). Their average value at canopy level decreased significantly in treated

samples with respect to controls after 1 day of treatment, as net CO₂ assimilation. Besides vegetation photosynthetic activity F_{s760} responds to the magnitude of incident PPFD which varies from day to day because of different atmosphere optical properties. On the contrary, NF_{s760} , being normalized by the magnitude of incident radiation, is more stable during the course of the experiment (Figure 4b).

A greater recourse to photoprotective mechanisms in treated samples with respect to controls is shown by PRI from day 3 (Figure 4c) when ozonated plants activate the xanthophyll cycle to protect the photosynthetic apparatus from the excess energy absorbed as observed by other authors [42-44].

Figure 4. Time series of spectral variables measured at 10:30 a.m. (solar time): (a) solar-induced steady-state fluorescence at 760 nm (F_{s760}); (b) normalized fluorescence at 760 nm (NF_{s760}); (c) Photochemical Reflectance Index (PRI); (d) Normalized Difference Vegetation Index (NDVI). Full and empty dots refer to control and treatment samples respectively. Values represent means \pm SE ($n = 3$). Comparison between means was performed according to Student's t-test (ns : $P > 0.05$; * : $P \leq 0.05$; ** : $P \leq 0.01$; *** : $P \leq 0.001$).



NDVI in treated samples showed significantly lower values on day 21 (Figure 4d) together with leaf level measurements of relative chlorophyll concentration (Figure 3d). The NDVI variation can be attributed to chlorophyll degradation, since, at the end of the experiment, structural variables affecting the index value were very similar (i.e. leaf dry matter content = 0.0030 and 0.0028 g cm⁻², LAI = 2.1 and 2.03 m² m⁻², in control and treated plants, respectively).

These results are in agreement with those of other authors [45, 46] thus indicating that traditional vegetation indices are sensitive to the damage phase of the stress, when chlorophyll concentration is altered and visible injuries have already occurred.

Briefly stated, it is shown that F_s and PRI measured at canopy level decreased significantly in treated plants as oxidative stress developed, thus confirming results previously observed at leaf level [47]. These results are in agreement with recent studies on RS detection of plant stress which showed a reduction in F_s and PRI values after prolonged oxidative stress [48-52]. It is also shown that NDVI decreased significantly with chlorophyll depletion and the appearance of visible injuries at the end of treatment.

5. Conclusions

In this research hyperspectral sensors were used to investigate the detection of ongoing plant stress by advanced RS techniques. A three-week O_3 fumigation experiment was conducted on potted white clover canopies. Physiological variables together with hyperspectral remote sensing measurements were collected.

Physiological measurements showed plant response to stress: net CO_2 assimilation and fluorescence quantum yield of treated samples were reduced with respect to controls after one and four days of fumigation, respectively. Maximum photochemical efficiency and relative chlorophyll concentration decreased significantly at the end of treatment when visible injuries occurred.

Spectral measurements acquired by two high spectral resolution spectrometers (FWHM = 0.13 and 2.8 nm, respectively) were used to calculate steady-state fluorescence variables (F_{s760} and NF_{s760}), PRI and NDVI.

Experimental data showed that the early phase of stress characterized by the decline of photosynthesis was successfully monitored by steady-state fluorescence variables (F_{s760} and NF_{s760}) which showed a significant decrease in plants exposed to O_3 after only one day of fumigation, similarly to net CO_2 assimilation. PRI values were significantly lower with respect to controls after three days of O_3 exposure. NDVI decreased significantly in the damage phase of stress (end of treatment) characterized by chlorophyll depletion and the appearance of visible symptoms.

Briefly stated, it was shown that recent hyperspectral RS methods that sense the energy dissipation pathways of the plant (i.e. steady-state fluorescence and PRI) are able to detect early stress symptoms of a generic oxidizing agent such as O_3 and can be integrated with traditional vegetation indices (i.e. NDVI) to monitor the evolution of plant response to stress.

Spectral measurements were conducted outdoors, under natural environmental conditions, with commercial high resolution field spectrometers to demonstrate that this technique is not confined to laboratory measurements but is promising for landscape level applications, using digital images acquired with airborne or satellite hyperspectral sensors.

A global satellite mission for sensing solar-induced fluorescence is currently under evaluation (ESA-FLEX, European Space Agency-FLuorescence EXplorer, [53]) and will open interesting perspectives for the early detection of plant stress at landscape level. However, upscaling of these methodologies still requires investigation on challenging issues such as the precise correction of atmospheric effects that might influence the estimation of steady-state fluorescence variables and PRI,

recently proven feasible on MERIS satellite data by Guanter *et al.* [54]. A better understanding of the influence of canopy structure, background and viewing geometry on PRI and steady-state fluorescence signals is also needed in order to map these variables in natural ecosystems with heterogeneous ecological characteristics. The recent availability of an integrated leaf-canopy fluorescence model (ESA, FluorMOD project, [55]) should provide the necessary tool for investigating these interactions by means of the simulation of canopy reflectance and fluorescence signals for varying canopy variables and viewing geometries.

Acknowledgements

The staff of the G. Scaramuzzi Department of Tree Science, Entomology and Plant Pathology, University of Pisa, Italy, is acknowledged for their help with the fumigation facility. We thank F. Fava for his support during the field campaigns. This research was supported by the Regione Lombardia INFOGESO project and by the Italian MIUR-PRIN 2005 project.

References and Notes

1. Lichtenthaler, H.K. The stress concept in plants: an introduction. In *Stress Of Life: From Molecules To Man*; Csermely, P., Ed.; *Ann. NY Acad. Sci.* **1998**; pp. 187-198.
2. Zarco-Tejada, P.J.; Miller, J.R.; Mohammed, G.H.; Noland, T.L.; Sampson, P.H. Vegetation stress detection through chlorophyll *a + b* estimation and fluorescence effects on hyperspectral imagery. *J. Environ. Qual.* **2002**, *31*, 1433-1441.
3. Sampson, P.H.; Zarco-Tejada, P.J.; Mohammed, G.H.; Miller, J.R.; Noland, T.L.; Fleming, R.L. Hyperspectral remote sensing of forest condition: estimation of chlorophyll content in tolerant hardwoods. *For. Sci.* **2003**, *49*, 381-391.
4. Coops, N.C.; Stone, C.; Culvenor, D.S.; Chisholm, L. Assessment of crown condition in eucalypt vegetation by remotely sensed optical indices. *J. Environ. Qual.* **2004**, *33*, 956-964.
5. Rossini, M.; Panigada, C.; Meroni, M.; Colombo, R. Assessment of oak forest condition based on leaf biochemical variables and chlorophyll fluorescence. *Tree Physiol.* **2006**, *26*, 1487-1496.
6. Baret, F.; Houlès, V.; Guéris, M. Quantification of plant stress using remote sensing observations and crop models: the case of nitrogen management. *J. Exp. Bot.* **2007**, *58*, 869-880.
7. Björkman, O.; Demmig-Adams, B. Regulation of photosynthetic light energy capture, conversion, and dissipation in leaves of higher plants. In *Ecophysiology of Photosynthesis*; Schulze, E.D., Caldwell, M.M., Ed.; Springer-Verlag: Berlin, **1995**; pp. 17-47.
8. Govindjee Chlorophyll *a* fluorescence: a bit of basics and history. In *Chlorophyll *a* Fluorescence: A Signature of Photosynthesis. Advances in Photosynthesis and Respiration*; Papageorgiou, G.C., Govindjee, Ed.; Springer: Dordrecht, **2004**; Vol. 19, pp. 1-42.
9. Apel, K.; Hirt, H. Reactive oxygen species: oxidative stress and signal transduction. *Ann. Rev. Plant Biol.* **2004**, *55*, 373-399.
10. Iriti, M.; Faoro, F. Oxidative Stress, the Paradigm of Ozone Toxicity in Plants and Animals. *Water Air Soil Poll.* **2008**, *187*, 285-301.
11. Plascyk, J.A. The MK II Fraunhofer line discriminator (FLD-II) for airborne and orbital remote sensing of solar-stimulated luminescence. *Opt. Eng.* **1975**, *14*, 339-346.

12. Moya, I.; Camenen, L.; Evain, S.; Goulas, Y.; Cerovic, Z.G.; Latouche, G.; Flexas, J.; Ounis, A. A new instrument for passive remote sensing 1. Measurements of sunlight-induced chlorophyll fluorescence. *Remote Sens. Environ.* **2004**, *91*, 186-197.
13. Meroni, M.; Colombo, R. Leaf level detection of solar induced chlorophyll fluorescence by means of a subnanometer resolution spectroradiometer. *Remote Sens. Environ.* **2006**, *103*, 438-448.
14. Elachi, C. *Introduction to the Physics and Techniques of Remote Sensing*; John Wiley and Sons: New York, **1987**; p. 63.
15. Plascyk, J.A.; Gabriel, F.C. The Fraunhofer Line Discriminator MKII- an airborne instrument for precise and standardized ecological luminescence measurements. *IEEE Trans. Instrum. Meas.* **1975**, *24*, 306-313.
16. Demmig-Adams, B.; Adams, W.W. Photoprotection and other responses of plants to light stress. *Ann. Rev. Plant Physiol. Mol. Biol.* **1992**, *43*, 599-626.
17. Horton, P.; Ruban, A.V.; Walters, R.G. Regulation of light harvesting in green plants. *Ann. Rev. Plant Physiol. Mol. Biol.* **1996**, *47*, 655-684.
18. Li, X.P.; Björkman, O.; Shih, C.; Grossman, A.R.; Rosenquist, M.; Jansson, S.; Niyogi, K.K. A pigment-binding protein essential for regulation of photosynthetic light harvesting. *Nature* **2000**, *403*, 391-395.
19. Horton, P.; Wentworth, M.; Ruban, A. Control of the light harvesting function of chloroplast membranes: The LHCII-aggregation model for non-photochemical quenching. *FEBS Lett.* **2005**, *579*, 4201-4206.
20. Yamamoto, H.Y. Biochemistry of the violaxanthin in higher plants. *Pure Appl. Chem.* **1979**, *51*, 639-648.
21. Bilger, W.; Björkman, O.; Thayer, S.S. Light-induced spectral absorbance changes in relation to photosynthesis and the epoxidation state of xanthophyll cycle components in cotton leaves. *Plant Physiol.* **1989**, *91*, 542-551.
22. Gamon, J.A.; Field, C.B.; Bilger, W.; Björkman, O.; Fredeen, A.L.; Peñuelas, J. Remote-sensing of the xanthophyll cycle and chlorophyll fluorescence in sunflower leaves and canopies. *Oecologia* **1990**, *85*, 1-7.
23. Gamon, J.A.; Peñuelas, J.; Field, C.B. A narrow-waveband spectral index that tracks diurnal changes in photosynthetic efficiency. *Rem. Sens. Environ.* **1992**, *41*, 35-44.
24. Nali, C.; Pucciariello, C.; Mills, G.; Lorenzini, G. On the different sensitivity of white clover clones to ozone: Physiological and biochemical parameters in a multivariate approach. *Water Air Soil Poll.* **2005**, *164*, 137-153.
25. Kärenlampi, L.; Skärby, L. Critical levels for ozone in Europe: testing and finalizing the concepts. *UN-ECE Workshop Report*, Kärenlampi, L., Skärby, L., Ed.; University of Kuopio, Department of Ecology and Environmental Science: Kuopio, Finland, **1996**.
26. Amoros-Lopez, J.; Gomez-Chova, L.; Vila-Frances, J.; Calpe, J.; Alonso, L.; Moreno, J.; del Valle-Tascon, S. Study of the diurnal cycle of stressed vegetation for the improvement of fluorescence remote sensing. In *Remote Sensing for Agriculture, Ecosystems, and Hydrology VIII*; Owe, M., D'Urso, G., Neale, C.M., Gouweleeuw, B.T., Ed.; *Proc. SPIE*, **2006**, *6359*, 63590R.
27. Milton, E.J.; Rolling, E.M. Estimating the irradiance spectrum from measurements in a limited number of spectral bands. *Rem. Sens. Environ.* **2006**, *100*, 348-355.

28. Meroni, M.; Colombo, R. 3S: A novel program for field Spectrometry at Subnanometer Spectral resolution. *Comput. Geosci.-UK*. **2008**, submitted.
29. Meroni, M.; Colombo, R.; Cogliati, S. High resolution leaf spectral signature for the detection of solar induced chlorophyll fluorescence. *Proc. 2nd Int. Workshop Rem. Sens. Veget. Fluores.* ESA Publications Division, Canadian Space Agency: Montreal, QC, Canada, **2004**.
30. Genty, B.; Briantais, J.M.; Baker, N.R. The relationship between the quantum yield of photosynthetic electron transport and quenching of chlorophyll fluorescence. *BBA* **1989**, *990*, 87-92.
31. Hayes, F.; Mills, G.; Harmens, H.; Novak, K.; Williams, P. *ICP Vegetation experimental protocol for monitoring the incidences of ozone injury on vegetation*. Natural Environment Research Council: Bangor, U.K., **2006**. Available from icpvegetation.ceh.ac.uk.
32. Guidi, L.; Nali, C.; Ciompi, S.; Lorenzini, G.; Franco, G. The use of chlorophyll fluorescence and leaf gas exchange as methods for studying the different responses to ozone of two bean cultivars. *J. Exp. Bot.* **1997**, *48*, 173-179.
33. Calatayud, A.; Ramirez, J.W.; Iglesias, D.J.; Barreno, E. Effects of ozone on photosynthetic CO₂ exchange, chlorophyll *a* fluorescence and antioxidant systems in lettuce leaves. *Physiol. Planta.* **2002**, *116*, 308-316.
34. Calatayud, A.; Iglesias, D.J.; Talón, M.; Barreno, E. Effects of 2-month ozone exposure in spinach leaves on photosynthesis, antioxidant systems and lipid peroxidation. *Plant Physiol. Biochem.* **2003**, *4*, 839-845.
35. Guidi, L.; Degl'Innocenti, E.; Genovesi, S.; Soldatini, G.F. Photosynthetic process and activities of enzymes involved in the phenylpropanoid pathway in resistant and sensitive genotypes of *Lycopersicon esculentum* L. exposed to ozone. *Plant Sci.* **2005**, *168*, 153-160.
36. Degl'Innocenti, E.; Guidi, L.; Soldatini, G.F. Effects of elevated ozone on chlorophyll *a* fluorescence in symptomatic and asymptomatic leaves of two tomato genotypes. *Biol. Planta.* **2007**, *51*, 313-321.
37. Paoletti, E. Ozone impacts on forests. *CAB Rev.: Persp. Agric. Vet. Sci. Nutr. Nat. Resour.* **2007**, *2*, 1-13.
38. Krause, G.H. Photo-inhibition of photosynthesis. An evaluation of damaging and protective mechanisms. *Physiol. Planta.* **1988**, *74*, 566-574.
39. Reichenauer, T.G.; Goodman, B.A.; KostECKI, P.; Soja, G. Ozone sensitivity in *Triticum durum* and *Triticum aestivum* with respect to leaf injury, photosynthetic activity and free radical content. *Physiol. Planta.* **1998**, *104*, 681-686.
40. Soldatini, G.F.; Lorenzini, G.; Filippi, F.; Nali, C.; Guidi, L. Photosynthesis of two poplar clones under long-term exposure to ozone. *Physiol. Planta.* **1998**, *104*, 707-712.
41. Shavnin, S.; Maurer, S.; Matyssek, R.; Bilger, W.; Sheidegger, C. The impact of ozone fumigation and fertilization on chlorophyll fluorescence of birch leaves (*Betula pendula*). *Trees* **1999**, *14*, 10-16.
42. Castagna, A.; Nali, C.; Ciompi, S.; Lorenzini, G.; Soldatini, G.F.; Ranieri, A. Ozone exposure affects photosynthesis of pumpkin (*Cucurbita pepo*) plants. *New Phytol.* **2001**, *152*, 223-229.

43. Elvira, S.; Alonso, R.; Castillo, F.J.; Gimeno, B.S. On the responses of pigments and antioxidants of *Pinus halepensis* seedlings to Mediterranean climatic factors and long-term ozone exposure. *New Phytol.* **1998**, *138*, 419-432.
44. Ranieri, A.; Giuntini, D.; Ferraro, F.; Nali, C.; Baldan, B.; Lorenzini, G.; Soldatini, G.F. Chronic ozone fumigation induces alterations in thylakoid functionality and composition in two poplar clones. *Plant Physiol. Biochem.* **2001**, *39*, 999-1008.
45. Rudorff, B.F.T.; Mulchi, C.L.; Daughtry, C.S.T.; Lee, E.B. Growth and radiation use efficiency of wheat and corn grown under elevated ozone and carbon dioxide atmospheres. *Remote Sens. Environ.* **1996**, *55*, 163-173.
46. Kraft, M.; Weigel, H.J.; Mejer, G.J.; Brandes, F. Reflectance measurements of leaves for detecting visible and non-visible ozone damage to crops. *J. Plant Physiol.* **1996**, *148*, 148-154.
47. Meroni, M.; Picchi, V.; Rossini, M.; Cogliati, S.; Panigada, C.; Nali, C.; Lorenzini, G.; Colombo, R. Leaf level early assessment of ozone injuries by passive fluorescence and PRI. *Int. J. Remote Sens.* **2008**, in press.
48. Richardson, A.D.; Berlyn, G.P.; Gregoire, T.G. Spectral reflectance of *Picea rubens* (Pinaceae) and *Abies balsamea* (Pinaceae) needles along an elevational gradient, Mt. Moosilauke, New Hampshire, USA. *Am. J. Bot.* **2001**, *88*, 667-676.
49. Dobrowski, S.Z.; Pushnik, J.C.; Zarco-Tejada, P.J.; Ustin, S.L. Simple reflectance indices track heat and water stress-induced changes in steady-state chlorophyll fluorescence at the canopy scale. *Remote Sens. Environ.* **2005**, *97*, 403-414.
50. Pérez-Priego, O.; Zarco-Tejada, P.J.; Miller, J.R.; Sepulcre-Cantó, G.; Fereres, E. Detection of water stress in orchard trees with a high-resolution spectrometer through chlorophyll fluorescence in-filling of the O-2-A band. *IEEE T. Geosci. Remote* **2005**, *43*, 2860-2869.
51. Thorhaug, A.; Richardson, A.D.; Berlyn, G.P. Spectral reflectance of *Thalassia testudinum* (Hydrocharitaceae) seagrass: low salinity effects. *Am. J. Bot.* **2006**, *93*, 110-117.
52. Suárez, L.; Zarco-Tejada, P.J.; Sepulcre-Cantó, G.; Pérez-Priego, O.; Miller, J.R.; Jiménez-Muñoz, J.C.; Sobrino, J. Assessing canopy PRI for water stress detection with diurnal airborne imagery. *Remote Sens. Environ.* **2008**, *112*, 560-575.
53. Stoll, M.-P.; Buschmann, C.; Court, A.; Laurila, T.; Moreno, J.; Moya, I. The FLEX-Fluorescence Explorer mission project: motivations and present status of preparatory activities. *IGARSS03.* **2003**, *1*, 585-587.
54. Guanter, L.; Alonso, L.; Gómez-Chova, L.; Amorós, J.; Vila, J.; Moreno, J. Estimation of solar-induced vegetation fluorescence from space measurements. *Geophys. Res. Lett.* **2007**, *34*, L08401, doi:10.1029/2007GL029289.
55. Zarco-Tejada, P.J.; Miller, J.R.; Pedrós, R.; Verhoef, W.; Berger, M. FluorMODgui V3.0 - A Graphic User Interface for the Leaf and Canopy Simulation of Chlorophyll Fluorescence. *Comput. Geosci.-UK.* **2006**, *32* (5), 577-591.